REPORT DOCUMENTATION PAGE

Form Approved OMB No. 0704-0188

1. AGENCY USE ONLY (Leave blank)	2. REPORT DATE	3. REPORT TYPE AND DATES COVERED
	October 1993	Final Report

4. TITLE AND SUBTITLE

Design Study of a 25-60 MA Plasma Flow Discharge Experiment Driven by a High Current Explosive Magnetocumulative Generator

5. FUNDING NUMBERS

6. AUTHOR(S)

N.F. Popkov, A.S. Pikar, E.A. Ryaslov, V.I. Kargin, P.V. Mironychev, D.V. Kotel'nikov, P.V. Korolev

7. PERFORMING ORGANIZATION NAME(S) AND ADDRESS(ES)

All-Russia Scientific Research Institute of Experimental Physics (VNIIEF)
607200, Arzamas-16
Nizhni Novgorod Region, Russia

8. PERFORMING ORGANIZATION REPORT NUMBER

SPC-93-4039

9. SPONSORING/MONITORING AGENCY NAME(S) AND ADDRESS(ES)

EOARD
PSC 802 BOX 14
FPO 09499-0200

10. SPONSORING/MONITORING AGENCY REPORT NUMBER

SPC-93-4039

11. SUPPLEMENTARY NOTES

12a. DISTRIBUTION/AVAILABILITY STATEMENT	12b. DISTRIBUTION CODE
Unlimited	

13. ABSTRACT (Maximum 200 words)

A conceptual project is developed to provide the plasma flow discharge experiments at 25 - 60 MA currents supplied by a MC - generator. As a primary source, a commercial helical MC-generator C-320 is used, which powers four helical - coaxial generators. Each helical - coaxial generator is equipped with an explosive plasma switch providing current commutation on a load 5 mcsec before the generators stop operating. The generator impedance matching with the plasma flow discharge impedance is facilitated by high voltage cable transformer. A vacuum inductive storage and a diagnostic system are located in a shielded construction 8 meters from the MC - generators. The plasma flow discharge calculated current constitutes 60 MA in 5 mcsec powering period.

14. SUBJECT TERMS	15. NUMBER OF PAGES
	35
	16. PRICE CODE

17. SECURITY CLASSIFICATION OF REPORT	18. SECURITY CLASSIFICATION OF THIS PAGE	19, SECURITY CLASSIFICATION OF ABSTRACT	20. LIMITATION OF ABSTRACT
UNCLASSIFIED	UNCLASSIFIED	UNCLASSIFIED	UL

NSN 7540-01-280-5500

Standard Form 298 (Rev. 2-89)
Prescribed by ANSI Std. 239-18
298-102

SPR-93-4039

Russia Federation Ministry of Atomic Energy.

Russia Federation Nuclear Center

All- Russia Scientific Research Institute of Experimental Physics.

RFNC - VNIIEF Scientific Leader
V.N.Mikhajlov

RFNC - VNIIEF Director
V.A.Belugin

Head of Fundamental and Applied Research Department of VNIIEF
Bossamykin V.S.

Design Study of a 25 - 60 MA Plasma Flow Discharge Experiment Driven by a High Current Explosive Magnetocumulative Generator.

Part 1.
(progress report)

Authors:

Popkov N.F.
Pikar' A.S.
Ryaslov E.A.
Kargin V.I.
Mironychev P.V.
Kotel'nikov D.V.
Korolev P.V.

607200, Arzamas - 16, Nizhni Novgorod region,
Russia Federation
Fax: (83) 3054565
Telex: 151109 ARSA

1993 year

ABSTRACT

A conceptual project is developed to provide the plasma flow discharge experiments at 25 - 60 MA currents supplied by a MC - generator.

As a primary source, a commercial helical MC-generator C-320 is used, which powers four helical - coaxial generators. Each helical - coaxial generator is equipped with an explosive plasma switch providing current commutation on a load 5 mcsec before the generators stop operating. The generator impedance matching with the plasma flow discharge impedance is facilitated by high - voltage cable transformer. A vacuum inductive storage and a diagnostic system are located in a shielded construction 8 meters from the MC - generators. The plasma flow discharge calculated current constitutes 60 MA in 5 mcsec powering period.

SPC-93-4039

THESIS.

INTRODUCTION

This work aim is the conceptual project development to provide the experiments with plasma - flow discharge at to 60 MA currents powered by a MC - generator of VNIIEF experimental base.

Currently there exist capacitive storages of 10 MJ stored energy and higher based on both high - current batteries and on high - voltage Marx generators. One can not expect the increase in the capacitive storage energy resource as with $1-2 cost for one joule of a capacitive storage, the cost of 100 MJ facility will constitute > $100 M. In this case the building expenses, experiment preparatory expenditures and the restoration cost for the ruined load after the electric pulse are not accounted [1].

Lately, very intense development have acquired the studies of various ways for inductive storage commutation in pulsed power generation at 1 -10 TW level. Interesting results in the plasma - flow discharge (PFD) application for these goals as well as the toroids at 10 MA and higher current were obtained at Shiva Star facility designed in USA Air Force Phillips Laboratory [2].

For a long time in VNIIEF the magnetocumulative generators have been studied as being the most energy effective and high - current sources, so the experience in generator design and application as well as the current commutation devices is considerable [3]. The MC - generators facilitate more than 100 MJ electromagnetic energy production rather easily at densities by 100 -1000 times higher compared with the capacitive storages.

The one joule cost in the explosive energy system comprising a MC - generator, a pulse shapes and a load is nearly $\$5.10^{-3}$, and for less than 100 pulses operation the explosive systems are more preferable than the capacitive storages in practical applications.

For the inductive storages powered by MC -generators as commutators capable to provide > 10 TW level, the electrically exploding wires, explosive foil and plasma commutators are employed.

Mainly the MC - generator application is limited because of load destruction with HE fragments and explosion products in each pulse and, consequently the energy obtained can not be used efficiently and the experiment is low informative due to the complexity in numerous measurement techniques' arrangement.

This drawback can be eliminated and the experiment can be made cheaper due to the VNIIEF designed and implemented technology for the explosive experiment, when the most expensive facility component, a load, is located in the shielded building, and the only damaged parts are a MC - generator placed in the firing field and a section of high - voltage cable line.

In this case as in the capacitive storages also, the capital expenses are required for a shielded building construction. However, with >10 pulse the one joule cost becomes less in this scheme at 100 MJ energy resource than the energy cost in the capacitive storage.

This report describes the PFD powering system employing the experiment technology based on MC - generators as energy sources, current contour breakage by a plasma commutator and preservation of the basic facility components in the special shielded construction.

The report consists of two parts: the first part is the analysis of various ways and scheme choice for experiment conduct aiming at PFD powering by MCG with 25-60 MA current; the second one is a more detailed description of all basic units in the facility, including MC-generators, explosive plasma commutator, pulsed high-voltage transformer, energy transmission line, vacuum inductive storage, PFD, load and diagnostic system.

1. ANALYSIS OF ENERGY TRANSFER SCHEME FROM INDUCTIVE STORAGE ON A LOAD.

In the experiment one needs to power a plasma flow switch with 60 MA current in 5 mcsec. If an energy transmission line insulated with solid-state polyethylene is used on the KVI-300 cable basis, the line voltage must not exceed 300 kV. The voltage pulse being triangle in the shape, the maximal magnetic flux stored in the cable line and storage facility does not exceed 0.8 Wb, thus the contour inductance must not be higher than 12 nH, correspondingly. The energy source must supply 22 MJ in the storage facility. Accounting the HE energy conversion efficiency to electromagnetic one which is not more than 10 % for MC-generators and this energy losses during its transmission to the storage, we have estimated the HE mass at 100 kg level. The HE of this mass must be at 5 m distance from the shielded construction, adding nearly 3 m more to the storage facility in the shielded building. Thus, the required length for the high-voltage cable line is 8 m.

If one distributes the inductance equally between the line and the storage, being 6 nH for each, then at 150 nH cable inductance per meter we shall obtain the needed number of cables in the line, i.e. 200 pieces.

To provide the required parameters of magnetocumulative generator powering, one can employ the energy transfer schematics shown in Fig.1 and 12.

The first schematic uses a high-voltage "high-speed" (5 mcsec is the effective time of flux output) MCG which supplies directly (or via a transformer) an inductive load. The second schematic employs a current opening switch for high-voltage pulse production. In this case MCG can be of low voltage (20-50 kV) and of (20-100 mcsec) characteristic operation time. Arbitrarily they can be named: a buffer inductance scheme and an opening switch scheme.

Let us consider the energy transmission efficiency on the inductive load in these schemes.

1.1. ENERGY TRANSMISSION VIA BUFFER INDUCTANCE.

To provide the demanded current rise time of 5 mcsec in the load one is forced to employ the high-voltage "high-speed" MC-generator and to switch on a load of MCG-operation, and to facilitate the generator powering and its operation one has to apply a buffer inductance at the current preamplification stage.

Fig.1 shows that load L_2 is switched via closing switch P on to the MC-generator L_0 with inductive storage L_1 in parallel to buffer inductance L_3.

During MC-generator operation, magnetic flux φ_2 is ousted from the decreasing to zero inductance L_0 to the load inductance

$$\varphi_2 = \frac{\varphi_0 L_p}{L_1 + L_p} , \qquad (1.1)$$

where $\varphi_0 = I_0 L_0$ - initial magnetic flux in MC-generator,

$L_p = \dfrac{L_2 L_3}{L_2 + L_3}$ - an equivalent inductance of the parallel coupling for a buffer and a load.

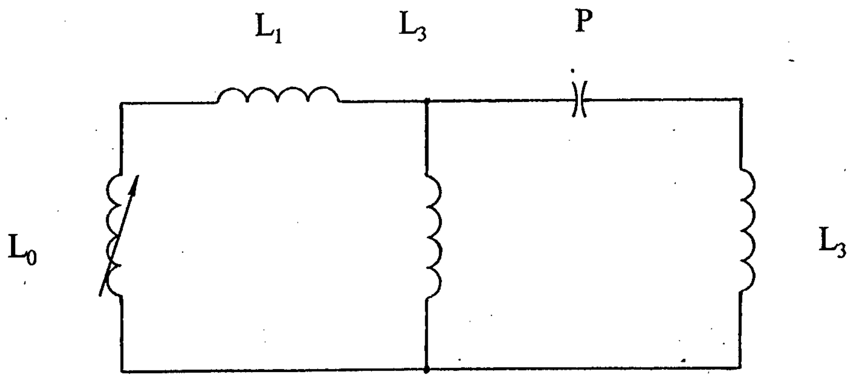

Fig.1. Buffer inductance scheme.

The magnetic flux in the storage inductance L_1 equals the sum of initial magnetic flux in storage and the flux portion ousted by the MC-generator:

$$\varphi_1 = I_0 L_1 + \frac{\varphi_0 L_1}{L_1 + L_p} , \qquad (1.2)$$

In the buffer inductance the magnetic flux will equal the sum of initial buffer magnetic flux and the additional flux equalling the load flux:

$$\varphi_3 = I_0 L_3 + \varphi_2 , \qquad (1.3)$$

The magnetic field energy in the inductance is defined with the formula:

$$W = \frac{\varphi^2}{2L} , \qquad (1.4)$$

The energy kept in inductance L1 is:

$$W_1 = \frac{\varphi_1^2}{2L_1} , \qquad (1.5)$$

The ratio of the energy kept in inductance L1 to the energy stored in the inductive load is:

$$\frac{W_1}{W_2} = \frac{L_1 L_2}{L_p^2}\left(1 + \frac{L_1 + L_p}{L_0}\right)^2 , \qquad (1.6)$$

The ratio of the energy lost in the buffer inductance to the energy stored in the inductive load will be:

$$\frac{W_3}{W_2} = \frac{L_2}{L_3}\left(\frac{\varphi_3}{\varphi_2}\right)^2 , \qquad (1.7)$$

By differentiating the given expression over the buffer inductance L_3 and equalling the obtained result to the zero, we shall find that the minimum ratio of the energy lost in the buffer inductance to the energy stored in the inductive load will be at:

$$L_3 = \frac{L_2 (L_0 + L_1)}{L_2 + L_1} , \qquad (1.8)$$

In this case the minimal ratio of the energy lost in the buffer inductance to the energy stored in the inductive load will be:

$$\frac{W_3}{W_2}/_{\min} = 4\frac{L_1 + L_2}{L_0} , \qquad (1.9)$$

With a rather large initial inductance of generator L_0 this schematic of energy transmission is highly efficient, however for "high-speed" generator of short operation time, L_0 and L_1 values can be compared to L_2 load inductance; and in the generator there is an order more energy kept than it is transmitted to the load and with account of the energy lost in the buffer inductance this schematic efficiency does not exceed some percent.

1.1.1. Conceptual Scheme and Calculated Parameters for High-Speed High-Voltage Explosive Magnetocumulative Generator to Power Inductive Storage with 30 MA Current in 5 mcsec.

Below a conceptual schematic and computed parameters are presented for the generator with buffer inductance to power the inductive storage PFD (20 nH) directly via the cable line (10 nH) with 30 MA current in 5 mcsec. Fig.2 displays a general equivalent electric circuit.

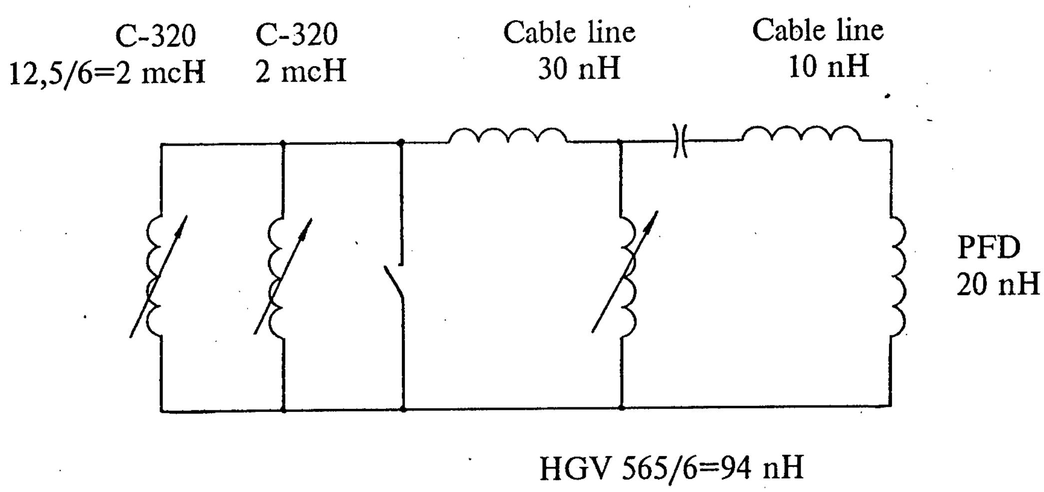

Fig.2. Equivalent electric circuit.

In spite of low efficiency in the energy transfer directly to the load, the similar schematic for PFD supply is attractive due to the fact that there is no any opening switches - the generator design provides for the short pulse formation.

Fig.3 presents the computed conceptual scheme for a high-voltage high-speed generator (HVG1). To withstand the required electric strength (nearly 300 kV), the generator stator is wound with a commercial high-voltage cable without a braid (a shield). At the generator output the cables form a transmission line nearly 4 m long to the inductive storage PFD.

The generator HVG1 is characterized with the following dimensions: outer diameter of a cable - 2.2 cm; central wire diameter - 10 mm; helix diameter - 50 cm; helix length - 75 cm.

The generator inductance at the moment of the armature expansion to the contact flanges (the flux capture) - 565 nH. The contact flanges are 46 cm in diameter.

Till the flux capture, the generator is powered by two generators C-320 with nearly 8 MA current via the cable line and buffer inductance of almost 200 nH (together with the cables). Closing and opening switches are absent here.

The similar powering scheme has minimal number of elements.

To minimize the HE mass placed in the immediate vicinity of the load, two metallic liners are supposed to be used in the armature. Thus, we attain a reduced HE mass and increased velocity of the last liner that is important for the increased speed of generator operation and higher voltages. On the generator axis (see Fig.3) a copper tube is placed (a wall - 10 mm, outer diameter - 14 cm) with HE (1.735 g/ccm, D=8.15 km/sec). After a two-fold expansion the first liner acquires nearly 2 km/sec velocity. HE mass is 15 kg in one generator. At 14 cm radius the copper liner strikes against the aluminium cylinder liner and imparts 3 km/sec velocity and higher.

When this liner appeared at 23 cm radius, the contact flanges insulations are mechanically damaged, the flux is captured and the load circuit is closed. The generator stops operating when the aluminium liner strikes against the helix insulation. From the moment of current flow in the generator load, the second liner passes nearly 15 mm.

To obtain 30 MA current in the load (30 nH) one needs to couple 6 generators of the type described in parallel.

Figs. 4-7 give the calculated graphs for helix current, load current, cable voltage and energy for one generator.

The main approximations employed in the numerical model for all further described generators are the following. For the inductance computation of the sectioned helical generator, the axial magnetic field uniformity is supposed to be within each section. To account the edge and other effects resulting in the decrease of this inductance, a constant fitting coefficient, K, is introduced. The generator length element inductance with alternating turns' density and alternating radii for a stator and an anchor is of the form:

$$dL = \frac{\mu_0}{2\pi}\left[2\pi^2 n^2 K\left(R_s^2 - R_a^2\right) + \ln\frac{R_s}{R_a}\right]dZ, \qquad (1.10)$$

where Rs - a stator radius, Ra - an armature radius, - turns' density. T[illegible] [illegible]termine K value, we have applied either more accurate 2-D inductance computations , or the results of its measurements with a generator model.

The skin-layer technique supports the generators' resistance calculations. The magnetic field distribution in the metal with conductivity σ is characterized by the skin-layer thickness

$$\delta = \sqrt{\frac{\tau}{\mu_0 \sigma}} \;, \qquad (1.11)$$

hear τ - characteristic rise - time for magnetic field.
The metal conductivity is chosen with joule heating account:

$$\sigma = \frac{\sigma_0}{1 + 0.5\alpha\beta\mu_0 H^2} \;, \qquad (1.12)$$

here $2/3 < \alpha < 1$ - a fitting coefficient,
β - a thermal coefficient of a metal,
σ_0 - initial conductivity,
H - magnetic field strength.

The generator armature motion is calculated at the end initiation in 1-D approximation of the independent cross-sections in the assumption of detonation

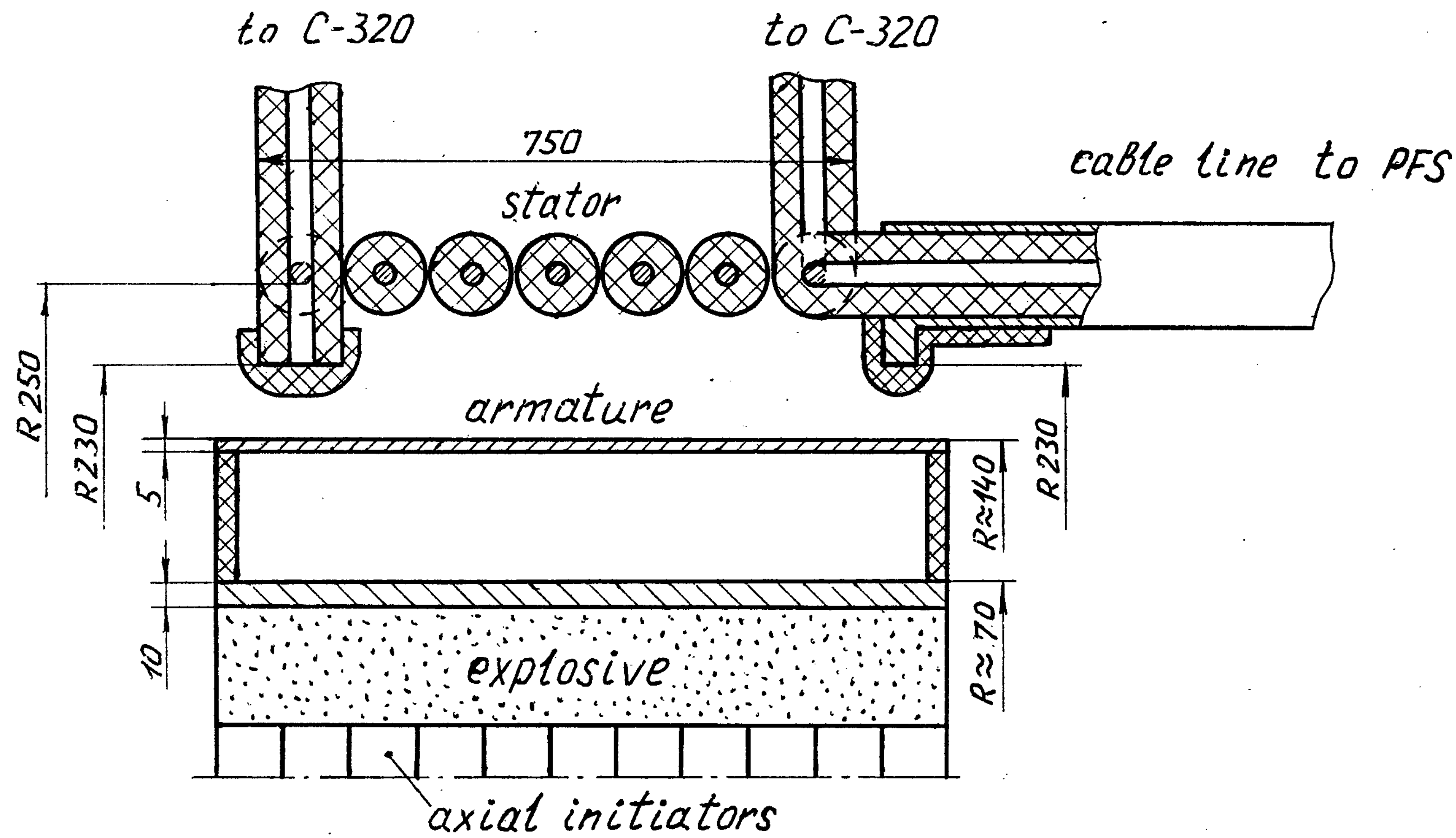

Fig. 3. Schematic of the short-pulse high-voltage explosive magnetic cumulative generator with simultaneous initiation (HVG1).

13:46:37 16-AUG-93 ПИКАРЬ

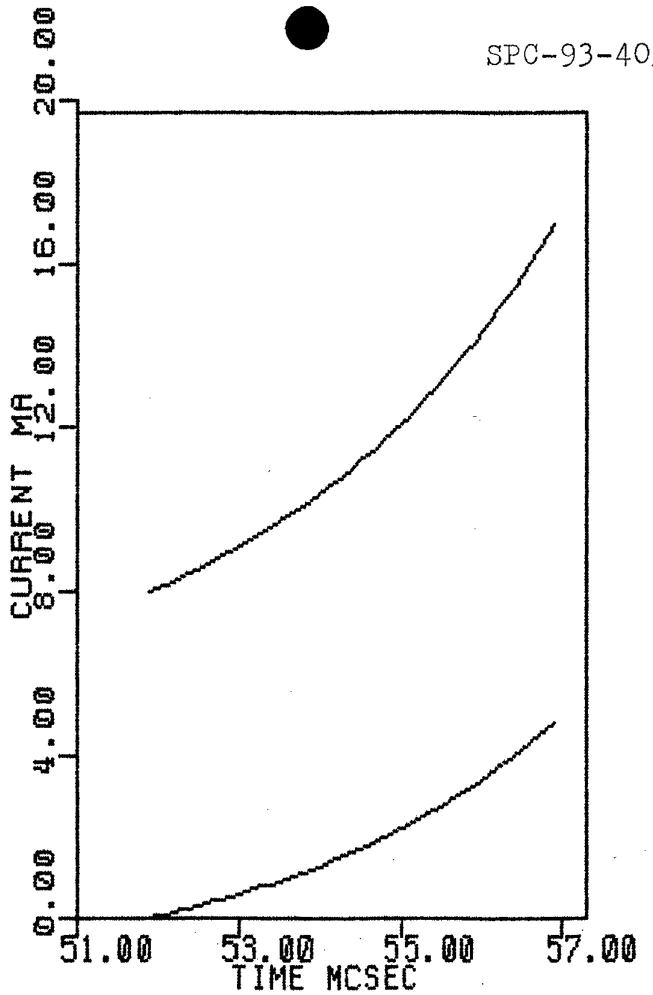

FIG.4. CALCULATED GENERATOR HVG1 COIL CURRENT JC, AND LOAD CURRENT JL, AFTER FLUX CAPTURE MOMENT.

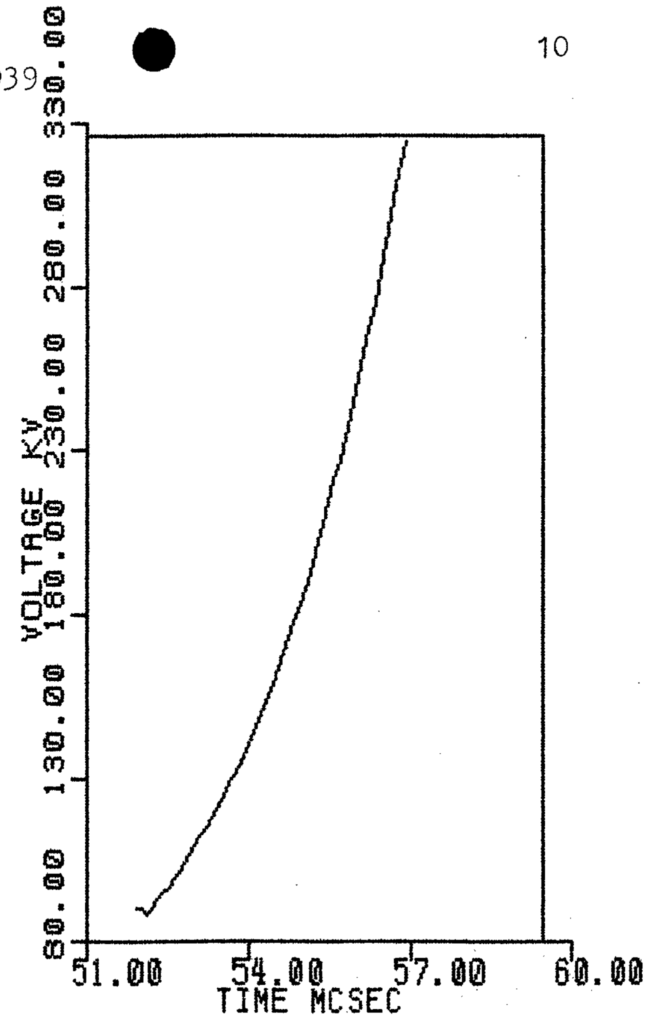

FIG.5. CALCULATED CABLE LINE VOLTAGE FOR HVG1.

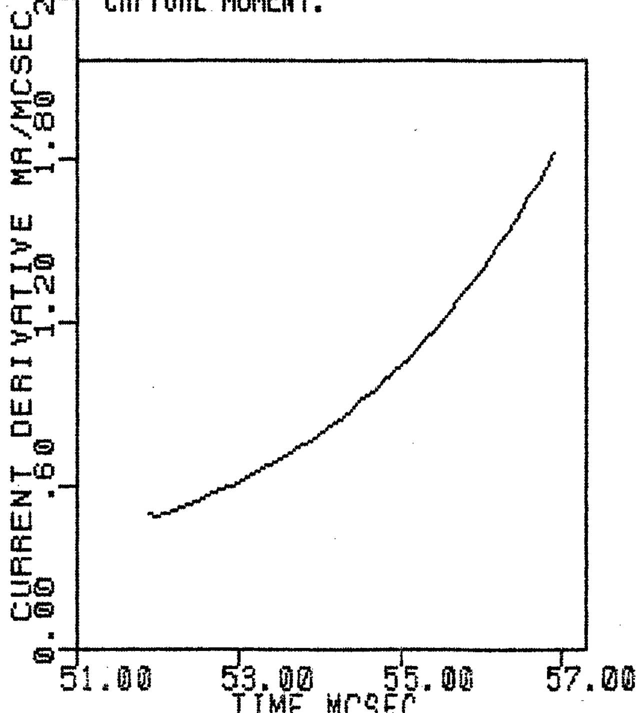

FIG.6. CALCULATED HGV1 LOAD CURRENT DERIVATIVE AFTER FLUX CAPTURE MOMENT.

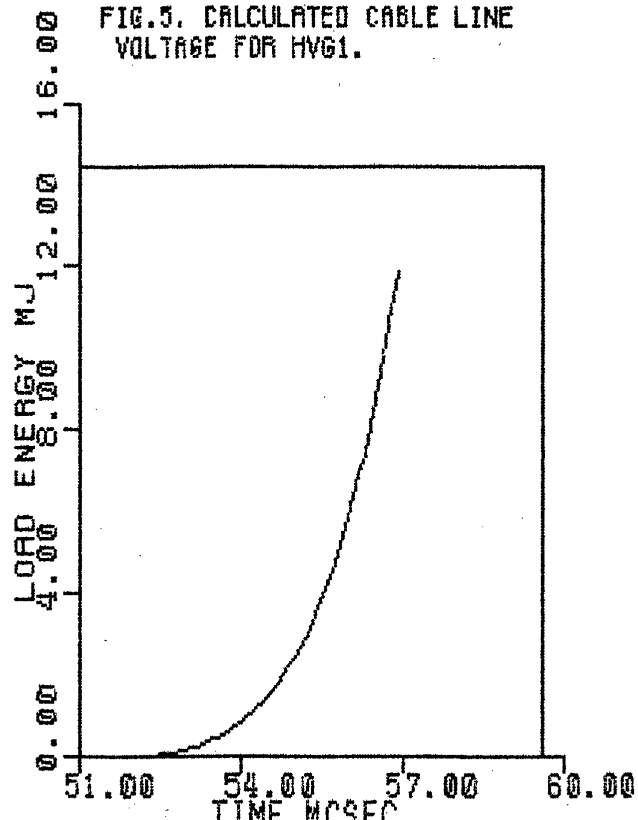

FIG.7. CALCULATED LOAD ENERGY FOR SIX HGV1 GENERATORS.

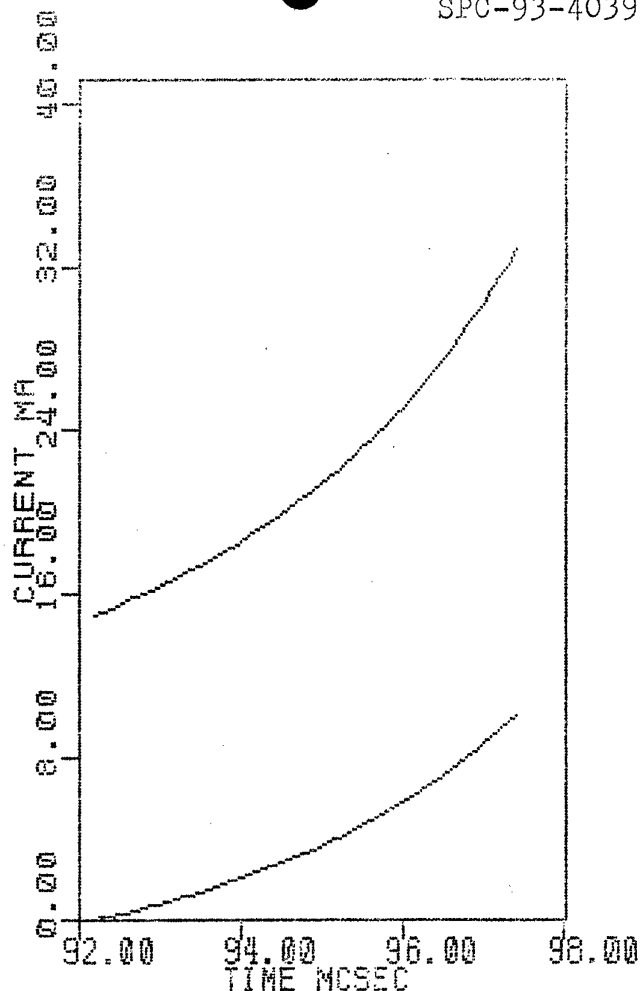

FIG.8. CALCULATED GENERATOR HVG2 COIL CURRENT JC, AND LOAD CURRENT JL, AFTER FLUX CAPTURE MOMENT.

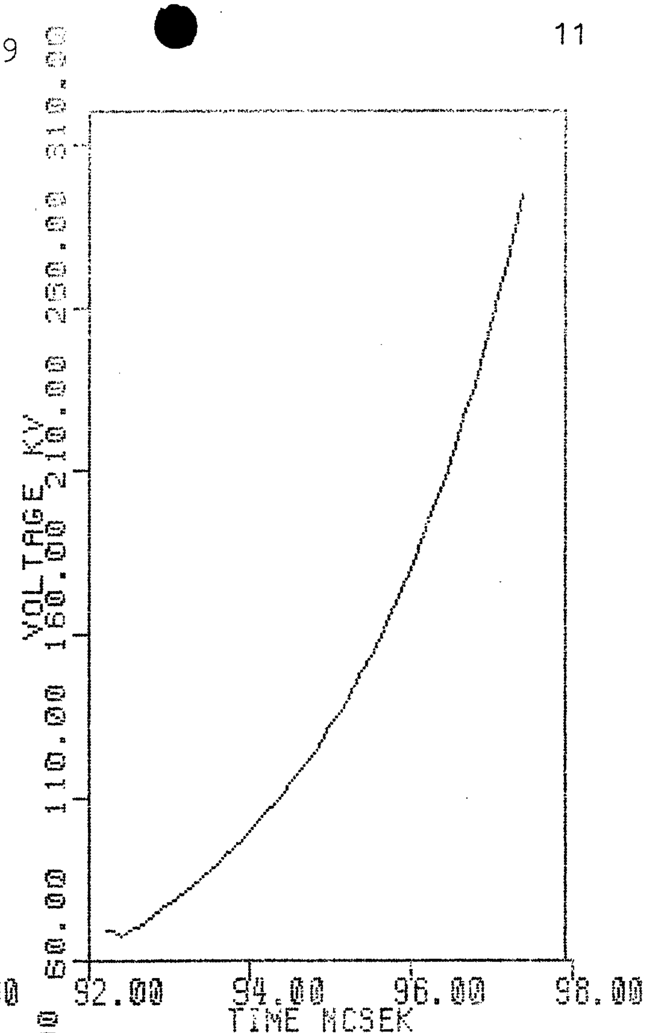

FIG.9. CALCULATED CABLE LINE VOLTAGE FOR HVG2.

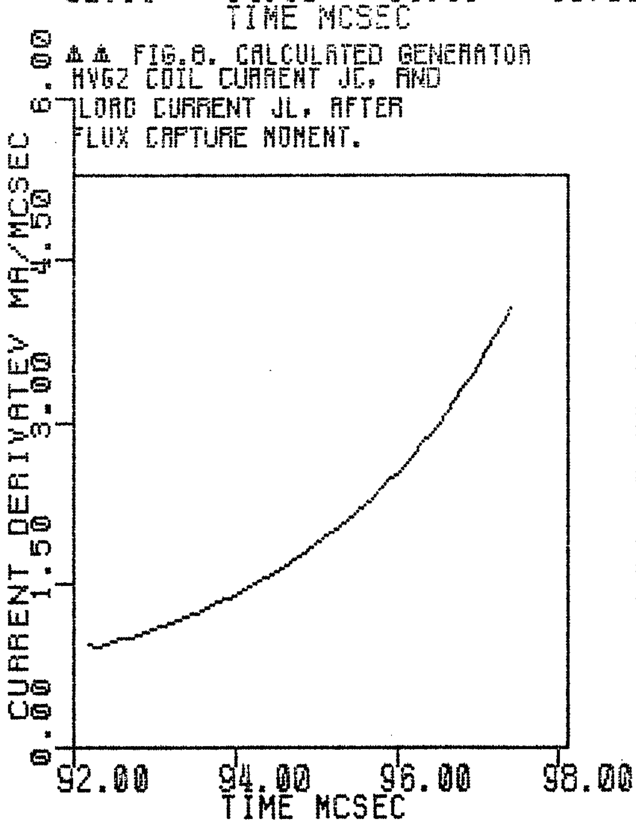

FIG.10. CALCULATED HVG2 LOAD CURRENT DERIVATIVE AFTER FLUX CAPTURE MOMENT.

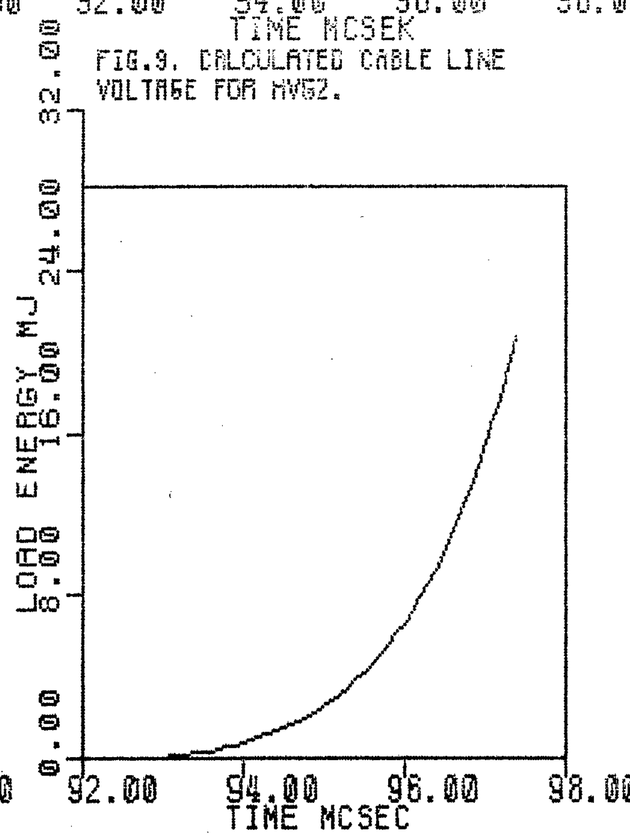

FIG.11. CALCULATED LOAD ENERGY FOR SIX HVG2 GENERATORS.

16-AUG-93 12:14:19

ПИКАРЬ

products uniformity over the radius, and with account of magnetic field pressure. In the generators with simultaneous axial initiation the approximations of experimental data and more accurate gas dynamic calculations are used.

1.1.2. Magnetocumulative Generator HVG2 Scheme and Computed Parameters to Power Inductive Storage Directly with 60 MA Current in 5 mcsec.

One can power the inductive vacuum storage with the plasma flow discharge to 60 MA current in 5 mcsec directly via the cable line with high-speed high voltage explosive magnetocumulative generators of HVG1 type already described (fig.3) but of somewhat larger size. In this case if the permissible cable voltage is 300 kV, the HVG2 generator load inductance (collectors +line +vacuum storage +plasma liner) will constitute nearly 12 nH.

The alternating inductance of the plasma link moving along the axis may be approximated with the expression:

$$L_p(t) = 2(t / \tau)^4 \text{ , nH,} \qquad (1.13)$$

where t - time after the load circuit closing;

T = 5 mcsec - powering period.

At 60 MA current and negligible resistance of the plasma, its voltage will be

$$U_p = \dot{L}(t)J(t) < 100 \text{ kV,} \qquad (1.14)$$

The number of HVG2 generators was chosen to be 6. Each generator is designed for 10 MA current, not higher. The preliminary calculations give the following HVG2 generator dimensions.

Helix diameter	80 cm
Helix length	100 cm
First liner diameter in the armature	20 cm
Second liner diameter in the armature	40 cm
Helix turn's number	20

At the flow capture moment the generator inductance is 310 nH. The first copper liner of the armature is 1.5 - 1.8 cm thick in the wall. After two-fold extension it acquires 2 km/sec velocity. Then it strikes the second lighter aluminium liner 5-6 mm thick and imparts 3-3.5 km/sec velocity to it. The load is commutated at the contact closure at 38 cm radius. Figures 8 - 11 present the calculated electric characteristics for HVG2 generator. One HVG2 generator is supposed to be powered with nearly 15 MA current via 100 nH buffer inductance with four generators C-320.

The total initial energy in HVG2 generator and buffer inductance will constitute 45 MJ. The electrical circuit for the powering procedure is similar to the one given in fig. 2. On concord with the preliminary calculations the HVG2 generator operates from the flow capture moment till the aluminium liner strikes against the 5.5 mm thick cable insulation. In this case the generator's residual inductance is nearly 100 nH. This estimate was obtained with a supposition that the aluminium liner preserves a precise cylindrical form. One can suppose that after the impact also the magnetic flow and additional energy will continue to be pushed out to the load due to a certain compression of the insulating dielectric layer .

The energy will stop growing further either after the liner has stopped or due to the insulation breakdown.

The results cited for the numerical calculations of the fast operating generator geometry and parameters with the buffer inductance show that the considerable energy is stored in the buffer with generator residual inductance. This leads to the necessity of the primary energy source application of a rather high energy resource. In this case it is 12-24 generators C-320.

1.2. ENERGY TRANSFER VIA OPENING SWITCH.

In the second scheme shown in fig.12, during MCG operation its inductance L0 decreases to a zero, and the flow is ousted to L_1 storage inductance. At the maximal current I_0 in the storage, the opening switch operates and with the increase in R(t) resistance the magnetic flux stored in L_1 inductance is redistributed between L_1 and L_2 inductances.

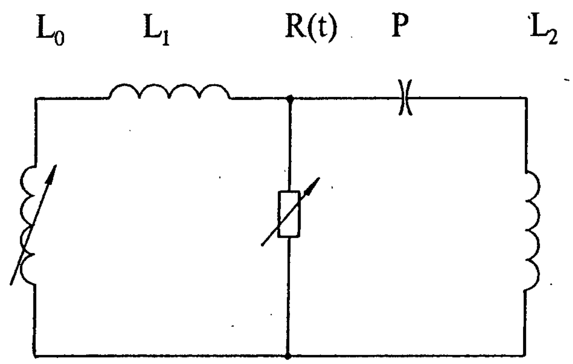

Fig.12. Opening switch scheme.

The magnetic flux in the load is:

$$\varphi_2 = I_0 L_1 / (L_1 + L_2), \qquad (1.15)$$

The magnetic field energy stored in the load equals:

$$W_2 = \varphi_2^2 / (2L_2), \qquad (1.16)$$

The energy left in L1 inductive storage equals:

$$W_1 = L_1 I_2^2 / 2, \qquad (1.17)$$

Then the ratio of the energy lost in L1 storage to the energy stored in the load inductance will be:

$$\frac{W_1}{W_2} = \frac{L_1}{L_2}, \qquad (1.18)$$

The energy dissipated by the opening switch will be estimated as:

$$W_3 = I_0 \varphi_2 / 2, \qquad (1.19)$$

Then the ratio of the energy lost in the opening switch to the energy stored in the load inductance will equal:

$$\frac{W_3}{W_2} = \frac{L_2}{L_1} + 1, \qquad (1.20)$$

As this formula depicts the energy dissipated in the opening switch is always larger than the energy stored in the inductive load at any ratio between L_1 and L_2.

1.2.1. Schematic and calculated parameters for slow-operating explosive magnetic generator SG to power the PFD storage via explosive plasma commutator with 30 MA current in 5 microseconds.

One can propose different conceptual schemes for energy facilities to produce 30 MA 5 mcsec current pulse in 30 nH inductive storage. For example, the parallel cascades of helical explosive magnetocumulative generators can serve the energy base. At the cascade final stage the fast-operating (5 mcsec), high-voltage (300 kV), high-current (5-10 MA) explosive magnetic generators are mounted to transmit an impulse directly via the high-voltage cable line to the PFD storage. One can expect some difficulties to arise in the implementation of this scheme. Among them we can mention a low coefficient of HE energy transformation in the payload energy that leads if the energy is big, to the necessity of large HE masses (100 kg) concentration in the immediate vicinity to the load.

Currently, a more real seems a scheme with a cascade of slow enough and low-voltage magnetocumulative generators to power the explosive plasma commutators (EPC) which provide the required current pulse generator in the storage PFD.

It is important to note that there is enough experience in 10 MA current pulse generation in 1-10 mcsec with such commutators [3]. Fig.13 presents the equivalent electric circuit for the facility containing EPC.

C-320 + SG   line R_{epc} P   PFD

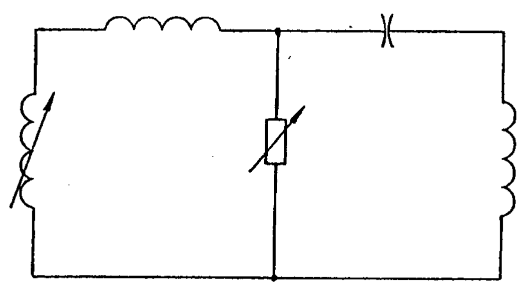

Fig. 13. Electrical scheme for energizing PFD with cascade generators and explosive driven plasma open switch.

The cascade of generators C-80, C-160, C-320 (further only C-320) is powered by a capacitor bank (E = 1.5 kJ). The C-320 powers three SG generators in parallel, which parameters are described below.

The C-320 cascade is well elaborated experimentally and provides 10^4 energy amplifier coefficient [4,6,7].

Fig.14 gives the experimental characteristics for C-320 cascade. In each SG generator the C-320 facilitates 1.3-1.5 MA initial current and 2.2 MJ initial energy. At the end of C-320 operation its current increases by e-times in 80 mcsec.

The explosive magnetic generator SG is similar to the known C-320, C-320M [7], and also to Mark VIII [8], Mark IX [9]. They produce to 25 MJ energies and 20-25 MA currents. As it's seen in fig. 15, SG generator has a four sections, multiwire helical stator with a coaxial straight copper tube containing nearly 40 kg HE. The HE is initiated from the end. After its detonation a 12^0 angle moving cone is formed on the tube.

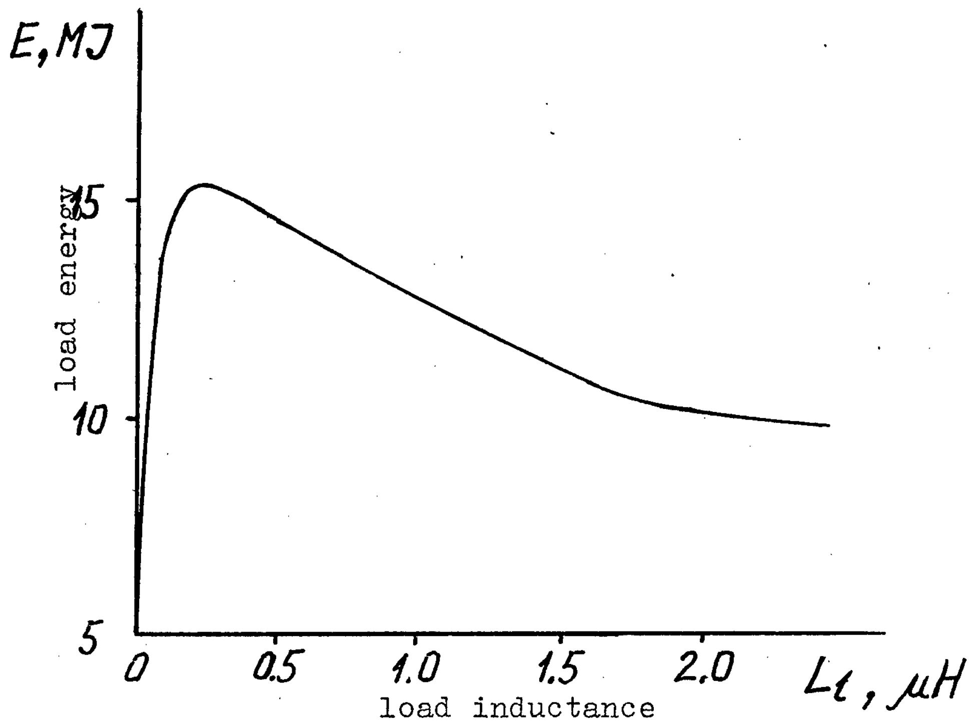

Fig. 14. Load energy generated by C-320 /4/.

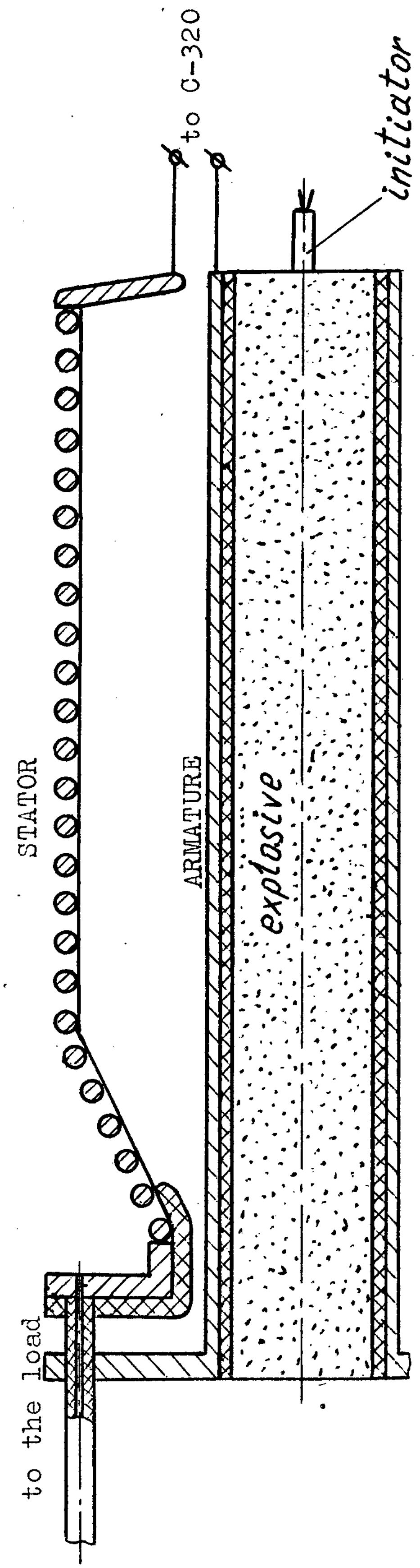

Fig. 15. Schematic of the SG generator.

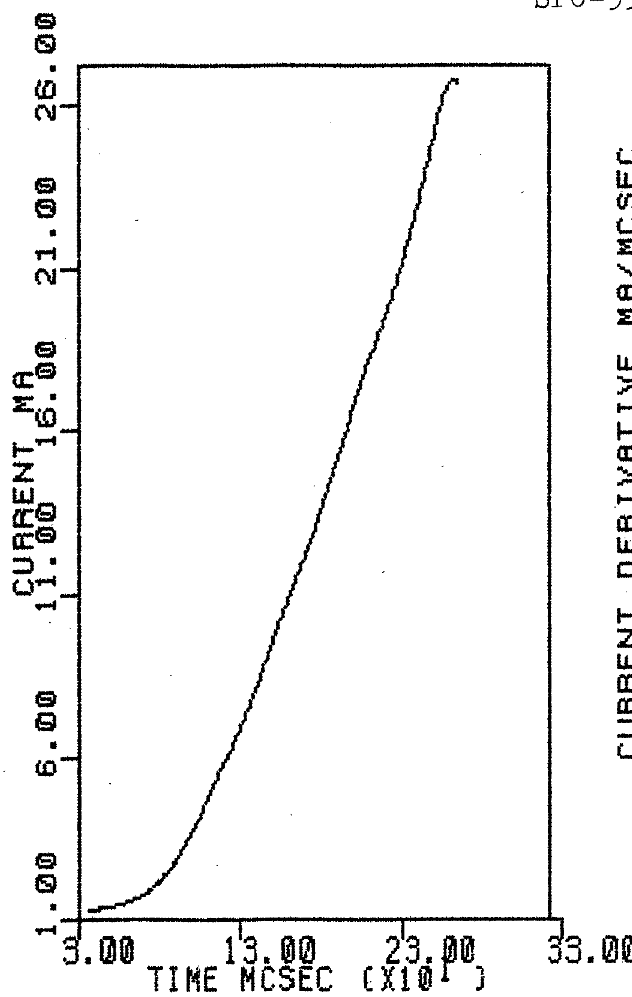

FIG.16. CALCULATED GENERATOR 5G CURRENT.

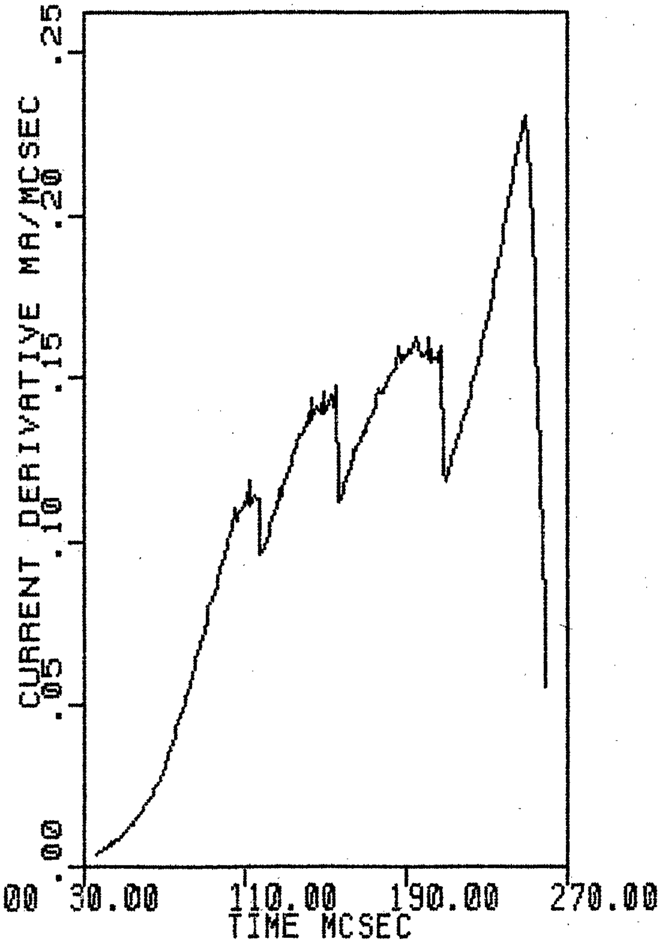

FIG.17. CALCULATED GENERATOR 5G LOAD CURRENT DIRIVATIVE.

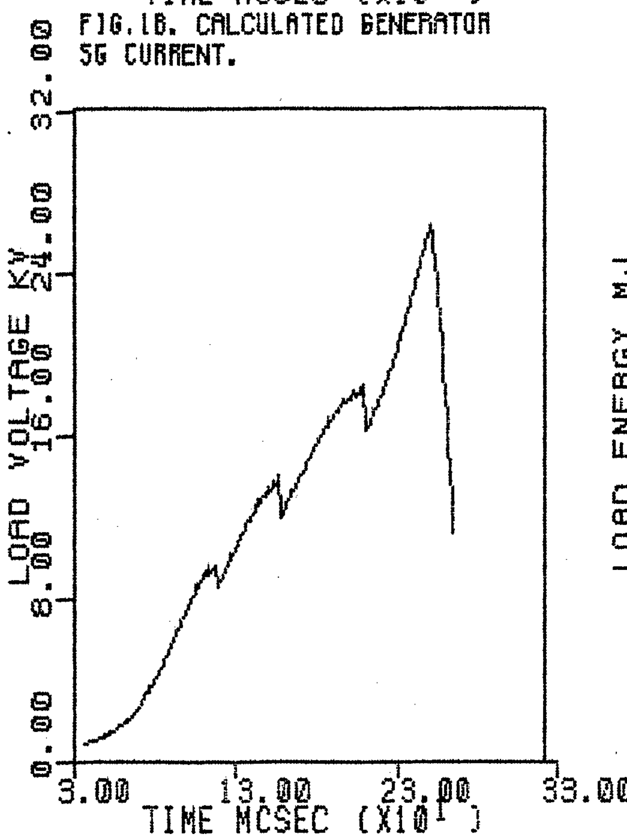

FIG.18. CALCULATED GENERATOR 5G LOAD VOLTAGE.

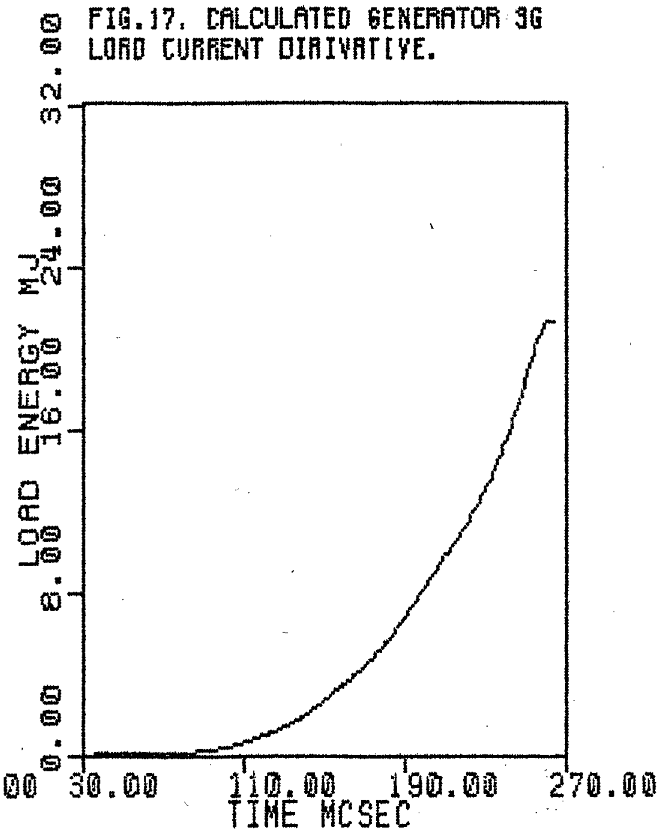

FIG.19. CALCULATED GENERATOR 5G LOAD ENERGY.

11:59:54 16-AUG-93 ПИКАРЬ

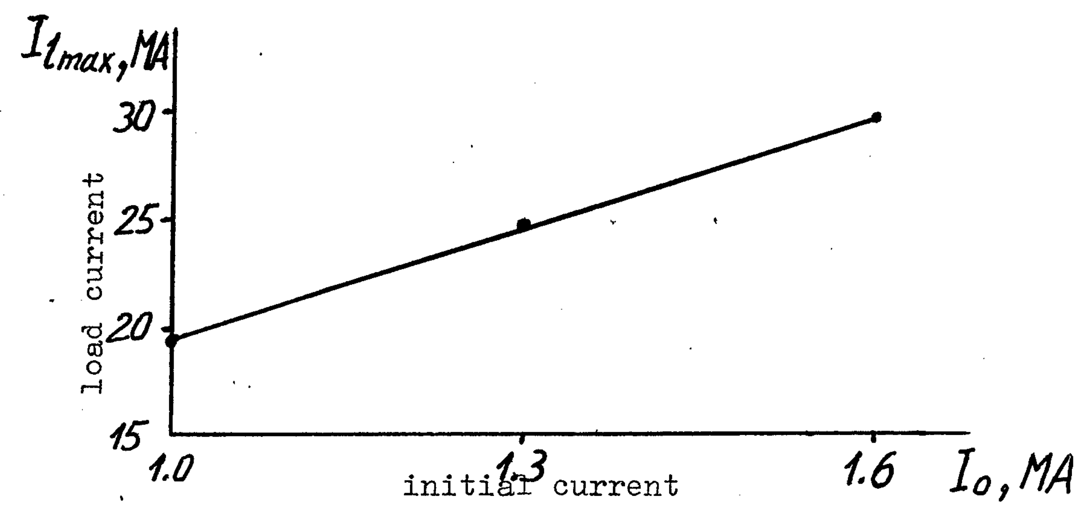

Fig. 20. Calculated SG generator current (load: 6o nH, 0.5 mOhm).

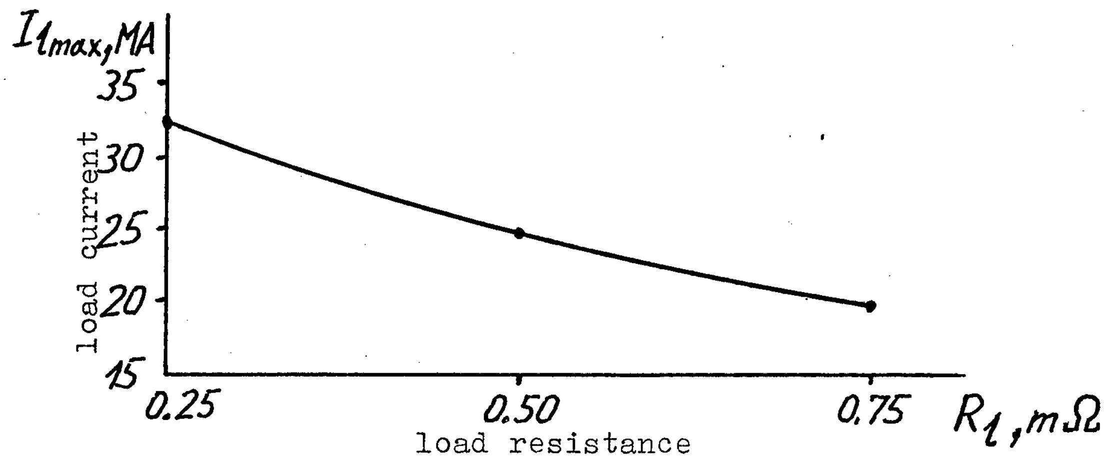

Fig. 21. Calculated SG generator current (60 nH load, J_o=1.3 MA).

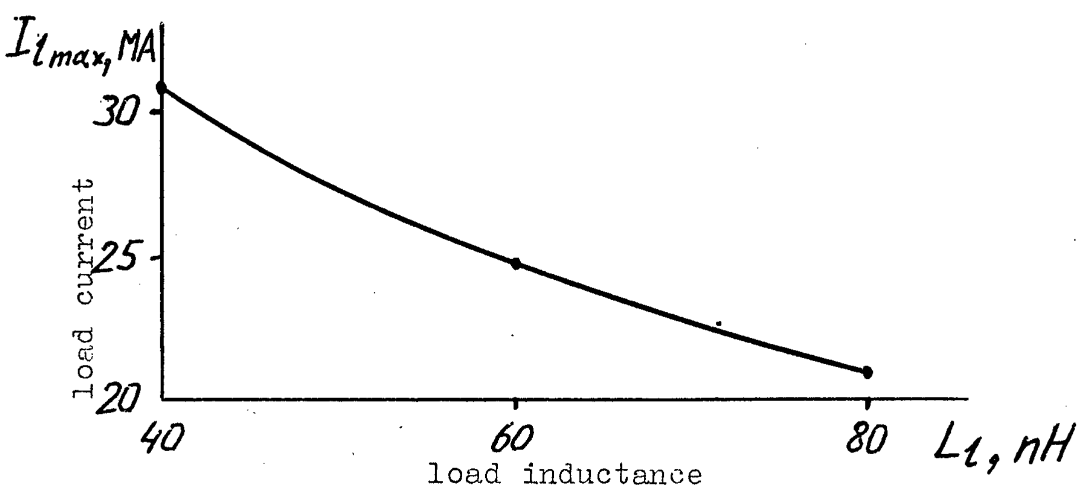

Fig. 22. Calculated SG generator current (0.5 mOhm load, J_o=1.3 MA).

The generator helix 32 cm in diameter and 190 cm long is mounted with insulated copper wires. A "bare" wire diameter - 10 mm, insulation thickness - 1.0 mm. The first generator section is of 8 parallel wires which double from section to section. Table 1 contains additional information on the section design. The generator inductance is nearly 2.6 μH at the capture moment. The flow is captured when the tube strikes against the contact at 11.5 cm radius. The generator armature is supposed to be made of a straight cylindrical copper tube 16 cm in outer diameter and 0.8 cm wall thickness. Between the HE and the metal a light tightening gasket is made of organic glass 0.8 cm thick.

Table 1.

Section	Length (cm)	Coil wires diameter (bare/insulated) (cm)	Number of parallel wires
1	30	1.0/1.2	8
2	30	1.0/1.2	16
3	40	1.0/1.2	32
4	64	1.0/1.2	64

In SG generator the initial flow is produced with a C-320 which powers three parallel SG generators of 4 - 4.5 MA total current. Each generator produces 3.5 Wb magnetic flux.

Figures 16 - 19 present calculated characteristics for SG generator operating on an inductive- ohmic load of constant parameters which simulates an explosive plasma commutator. The calculations were done with the program similar to the one described in ref. [10]. It satisfactorily describes the operation of Mark VIII [8,10], Mark IX [9], C-320 and C-320M [7] which are similar in the class and parameters.

Figures 20 - 22 illustrate the generator parameters dependence on supply current I, load inductance L and load resistance R. From the study results for explosive plasma commutators (EPC) [4,5] one can conclude that its ohmic resistance will be in the range of 0.2 - 0.5 Ohm in the considered powering regime. The fig. 21 load resistance variation are due to this.

1.3. SCHEME WITH CURRENT CONTOUR BREAKAGE AND SIMULTANEOUS MAGNETIC FLUX OUSTING BY MC-GENERATOR.

The above described scheme of the opening switch usage can be modified via its uniting with the first scheme.

In this scheme (fig. 23) the opening switch transmits the current to supply MCG and to preamplify current preliminary, and 5 mcsec before MC generator stops operating R opening switch resistance grows and simultaneously load L_2 is switched on the inductive storage L_1. The magnetic flux is ousted from the storage to the load by the MCG expanding liner.

By the end of MCG operation the magnetic flux is stored in the load inductance

$$\varphi_2 = I_0(L_0+L_1)L_2/(L_1+L_2), \qquad (1.21)$$

Then the energy stored in the load inductance equals, correspondingly:

$$W_2 = \frac{L_2 I_0^2}{2}\left(\frac{L_0+L_1}{L_1+L_2}\right)^2, \qquad (1.22)$$

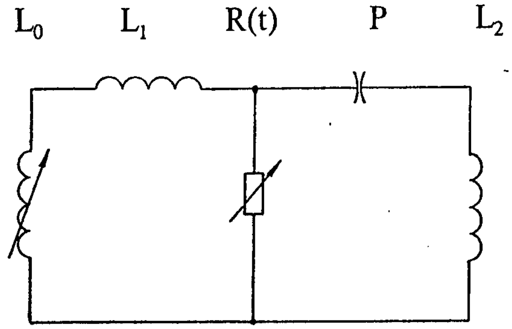

Fig.23. scheme with current contour breakage and simultaneous magnetic flux ousting.

At the MCG operation ending L_1 inductance current equals I_2 load current and the energy kept in L_1 inductive storage equals:

$$W_1 = L_1 I_2^2/2, \qquad (1.23)$$

Then the ratio of the energy lost in L_1 storage to the energy stored in the load inductance will be:

$$\frac{W_1}{W_2} = \frac{L_1}{L_2}, \qquad (1.24)$$

In this case the opening switch dissipates the energy:

$$W_3 = \frac{I_0 \varphi_2}{2} = \frac{I_0^2}{2} \frac{(L_0 + L_1) L_2}{(L_1 + L_2)}, \qquad (1.25)$$

The ratio of the energy lost in the opening switch to the energy stored in the load inductance will be:

$$W_3/W_2 = (L_1+L_2)/(L_1+L_0) \qquad (1.26)$$

As the given formula shows the energy transfer efficiency grows with the increase in the initial generator inductance, however for "fast-operating" generators of short operation time L_0 value can be compared with L_2 load inductance and the energy dissipated by the opening switch is not much less than the energy stored in the load.

Comparing three above considered schemes for energy transfer one can mention that the most effective scheme is "1.3" scheme. Scheme "1.2" has the losses twice as much as in "1.3" and by 10 times more than "1.1" scheme.

In the experiments on the explosive MCG energy transmission on the load placed in the special shielded construction, scheme efficiency is one of the basic parameters. Large energy losses demand larger HE mass to be employed to compensate them.

In this case to protect against the HE damage affects it is necessary to increase the energy transmission line length, and in order to preserve MCG load inductance one needs to increase the cable number that makes the experiment conduct more complex. Thus, in our project we will dwell on the most effective, although most complex scheme with the simultaneous current contour breakage and MCG ousting of the magnetic flux.

2. BASIC ELEMENTS CONSIDERATION.

2.1. PLASMA FLOW DISCHARGE MODEL.

To define the basic requirements to the projected system let us consider a simplified model for plasma flow discharge (PFD) dynamics shown in fig.24.

```
            _____________________________
                         ||
self magnetic            ||→ velocity
field                    ||
            _____________||______________
                     d - thickness
```

Fig.24. Conceptual scheme for PFD.

Let us assume that the current increase in the PFD is linear in time: $I(t) = I_m(t/T)$ and the plasma layer moves under the self magnetic field pressure according to the law:

$$\rho d \ddot{x} = \mu_0 H^2 / 2, \qquad (2.1)$$

where ρ - plasma density, d - its thickness, H - self magnetic field.

Substituting the expression for the magnetic field in the form:

$$H = H_m(t/T), \qquad (2.2)$$

where H_m - maximal magnetic field, T - PFD powering time.

Then, the law for PFD plasma motion is founded:

$$\ddot{x} = \frac{\mu_0 H^2}{2\rho d}\left(\frac{t}{T}\right)^2, \qquad (2.3)$$

Plasma acceleration is defined by:

$$A = \frac{\mu_0 H^2}{2\rho d}, \qquad (2.4)$$

the law is rewritten in the form:

$$\ddot{x} = A\left(\frac{t}{T}\right)^2, \qquad (2.5)$$

Integrating this expression over time we find the plasma liner velocity:

$$\dot{x} = A\frac{T}{3}\left(\frac{t}{T}\right)^3, \qquad (2.6)$$

Integrating once more over t we will find the distance passed by the plasma:

$$x = A\frac{T^2}{12}\left(\frac{t}{T}\right)^4, \qquad (2.7)$$

2.2. ANALYSIS OF ENERGY TRANSFER SCHEME FROM STORAGE TO LOAD.

As the plasma velocity variation law for PFD and the distance passed by the plasma during the powering procedure are known, we can respectively find its inductance and the derivative:

$$\dot{L}_s = \frac{\mu_0 h \dot{x}}{2\pi R} = \frac{\mu_0 h}{2\pi R} A \frac{T}{3}\left(\frac{t}{T}\right)^3, \qquad (2.8)$$

here, $\mu_0 = 4\pi 10^{-7}$ H/m

R - PFD mounting radius, h - PFD plasma layer height. Correspondingly, the PFD inductance is:

$$L_s = \frac{\mu_0 h}{2\pi R} A \frac{T}{12}\left(\frac{t}{T}\right)^4, \qquad (2.9)$$

Let us analyze this scheme from the point of energy transmission from the generator to the load.

By the end of MCG operation the generator magnetic flux is redistributed between L_1, L_2 and L_s according to the expression:

$$(L_0+L_1)I_0 = I_2(L_1+L_2+L_s), \qquad (2.10)$$

We find out that the load current is:

$$I_2 = I_0(L_0+L_1)/(L_1+L_2+L_s), \qquad (2.11)$$

Then the energy stored in the load inductance equals:

$$W_2 = \frac{(L_2+L_s)I_0^2}{2}\left(\frac{L_0+L_1}{L_1+L_2+L_s}\right)^2, \qquad (2.12)$$

The energy kept in L_1 inductive storage is:

$$W_1 = L_1 I_2^2/2, \qquad (2.13)$$

In this case the opening switch dissipates the energy:

$$W_3 = \frac{I_0 \varphi_2}{2} = \frac{I_0^2}{2}\frac{(L_0+L_1)(L_2+L_s)}{(L_1+L_2+L_s)}, \qquad (2.14)$$

The ratio of the energy lost in the opening switch to the energy stored in the load inductance will be:

$$W_3/W_2 = (L_1+L_2+L_s)/(L_1+L_0) \qquad (2.15)$$

As it is evident from this formula the PFD alternating inductance improves the efficiency of the generator energy transmission to the load. Let us consider in detail the obtained relationship. To reduce the losses it is necessary to decrease L_1 and to increase L_0. In the MC-generator the ratio of L_1 residual inductance to the initial generator inductance, L_0, is proportional to the ratio of the insulation thickness to the initial gap in the generator.

The insulation thickness:

$$d = U/E, \qquad (2.16)$$

where U - the voltage between the generator buses, E -insulation breakdown strength .

The initial distance between the generator buses equals the product of the liner velocity by the generator operation time.

$$h = VT, \quad (2.17)$$

here, V - liner velocity, T - generator operation time.

Let us find the ratio of the residual inductance L_1 to the generator initial inductance L_0 :

$$L_1/L_0 = U/(EVT), \quad (2.18)$$

As we see, to decrease L_1/L_0 ratio one must decrease the generator voltage, increase the liner velocity and generator operation time. These requirements contradict the conditions for the successful PFD powering which demands the decrease in powering time and the increase in the voltage, respectively.

To solve this contradiction there exist several ways:

1. The voltage between the generator buses can be reduced if one employs some generators coupled in series. Then, each generator voltage will be N- times less than the total voltage. However,. at such system output one must install the insulation for the total voltage which contributes additionally to L_1 inductance, such coupling scheme is usually used for disk MC-generators when a generator is assembled of several series disks.

2. The second way to solve this problem is to use a high-voltage step-up transformer at the low-voltage MC-generator output. The transformer implementation in the circuit somehow complicates the general schematic but in this case the possibility arises to match with a corresponding coefficient choice more precisely, - the impedance of relatively low resistance supply source, - an MC-generator being such, - with a high-resistance load, i.e. the plasma flow discharge.

2.3. CABLE TRANSFORMER SCHEME.

In our project we would consider a high-voltage cable transformer design wound with the same cable as the energy transmission line. The cable transformer has a very low - inductance primary winding and its design does not include high-voltage separation surfaces that considerably reduces the breakdown probability.

Fig.25 gives the design scheme for the cable transformer with two turns.

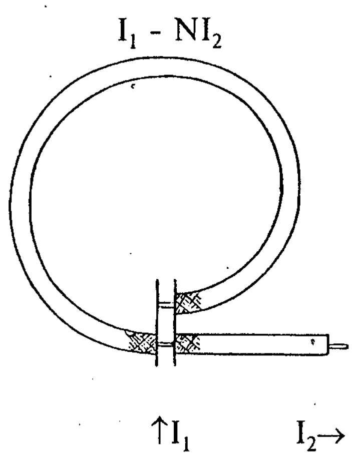

Fig.25. Cable transformer design scheme.

Let us designate the transformer input buses' current as I_1, the cable output current as I_2, then the cable braid outer side current will be:

$$I = I_1 - I_2 N, \quad (2.19)$$

where N - transformation factor equalling the number of cable rounds in the transformer.

The magnetic field energy in this transformer equals the sum of magnetic field energies between the input buses, in the cable and outside the cable in the transformer coil.

The magnetic field energy between the input transformer buses equals:

$$W_1 = \frac{\mu_0 h l d}{2}\left(\frac{I_1}{h}\right)^2, \tag{2.20}$$

where h - input buses' width, l - buses' length, d - gap between the buses.

The magnetic field energy in the cable is:

$$W_2 = \frac{\mu_0 \pi D(N-1)}{4\pi}\ln\left(\frac{R}{r}\right)I_2^2, \tag{2.21}$$

where D - transformer coil diameter; r, R - cable inner and outer radii; N - cable turns' number.

The magnetic field energy in the transformer coil is:

$$W_3 = \frac{\mu_0 \pi D^2 (N-1)R}{2}\left(\frac{I_1 - I_2 N}{2(N-1)R}\right)^2, \tag{2.22}$$

Let us introduce the designations

$$L_1 = \frac{\mu_0 l d}{h}, \tag{2.23}$$

$$L_2 = \frac{\mu_0 D(N-1)}{2}\ln\left(\frac{R}{r}\right), \tag{2.24}$$

$$L_3 = \frac{\mu_0 \pi D^2}{4(N-1)R}, \tag{2.25}$$

then the equivalent electrical transformer scheme reduced to a primary circuit is of the form shown in fig. 26.

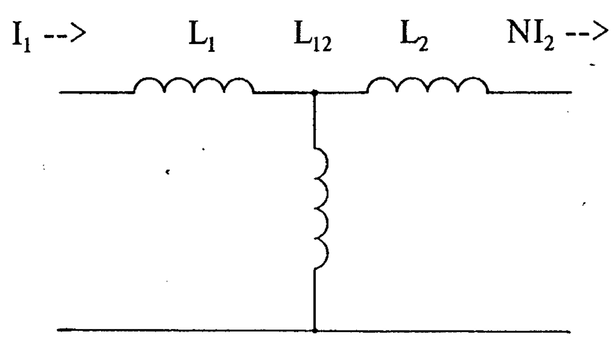

Fig. 26 Equivalent electrical transformer circuit.

The energy losses in transformer inductance L_{12} will be low compared to the energy in L_g load, when $L_{12} > L_2 + L_g/N^2$. This condition results in the fact that while choosing a transformer, one has to meet the requirement of $L_{12} >> L_2$ or using the above obtained expressions:

$$\frac{D}{2R} >> \frac{4}{\pi}\ln\frac{R}{r} \approx 1, \tag{2.26}$$

For the cable transformer this relationship is easily fulfilled as the coil diameter is always much larger than the cable diameter.

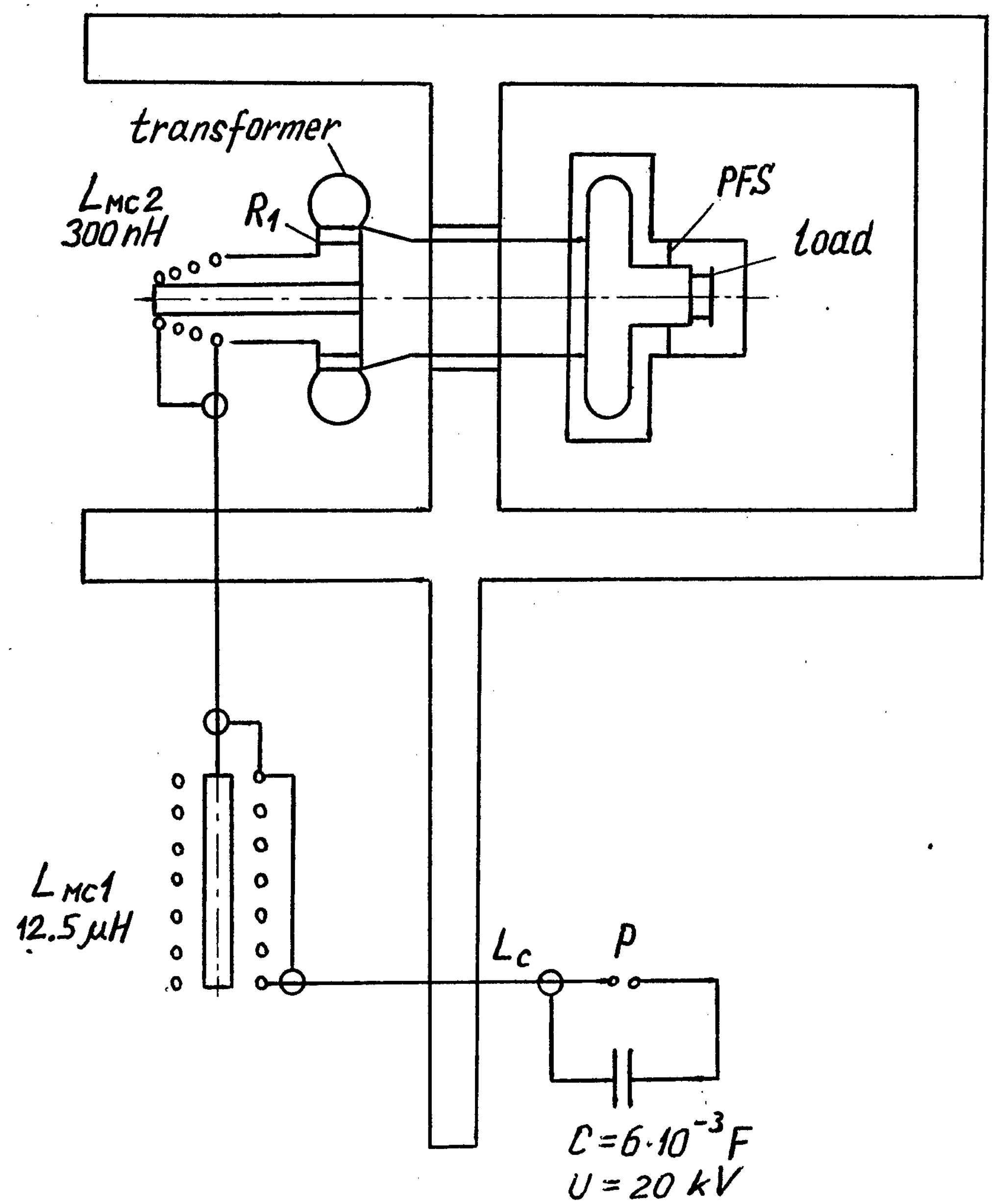

Fig. 27. Basic units arrangement in the facility.

3. ANALYSIS OF GENERAL ARRANGEMENT FOR EXPERIMENT.

After we have determined the basic components for the facility and main requirements to them, let us analyze the whole system operation. Basic units and their arrangement scheme are shown in fig. 27.

To power the preamplifier a capacitor bank C is used which is coupled via a switch P with a cable line Lc to MC generator Lmc1 of big operation time which serves as a preamplifier. This generator is needed to produce the initial magnetic field in the "high speed" MC generator Lmc2. For some time the "high-speed" MCG operates to the inductive storage, then 5 mcsec before it stops working the storage current contour is broken by the explosive plasma opening switch R1 and the circuit including a transformer, high voltage energy transformation cable line and PFD is switched on. During these 5 mcsec the "high speed" MC -generator ousts the magnetic flux from the generator residual inductance to the inductance of the cable line, vacuum storage and PFD.

Let us consider the operational consequence of basic units in the facility.

3.1. CAPACITOR BANK POWERING OF PREAMPLIFIER.

First, roughly the MC generator powering procedure with a capacitor bank can be shown in fig. 28 scheme.

Strictly speaking, resistance R and inductance L of the circuit vary in time, for example due to conductors' heating as well as magnetic field diffusion in the conductors. Their effects can be accurately accounted only in the numerical calculations, however for powering procedure analysis it is permissible to consider all components of the circuit shown in Fig.10 to be constant.

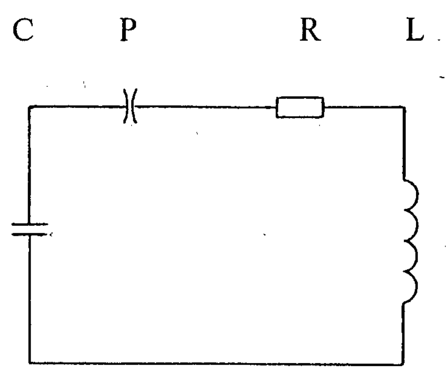

Fir.28. MC generator powering procedure with a capacitor bank.

Equation for the given circuit will be written in the following form:

$$L\dot{I} + RI + \frac{1}{C}\int I dt = U_0, \qquad (3.1)$$

with the initial condition of I(0)=0.

In the case of low attenuation at $R < 2\sqrt{\frac{L}{C}}$ the equation can be solved in the following way:

$$I = \frac{U_0}{\omega}\exp\left(\frac{-Rt}{2L}\right)\sin(\omega t), \qquad (3.2)$$

where

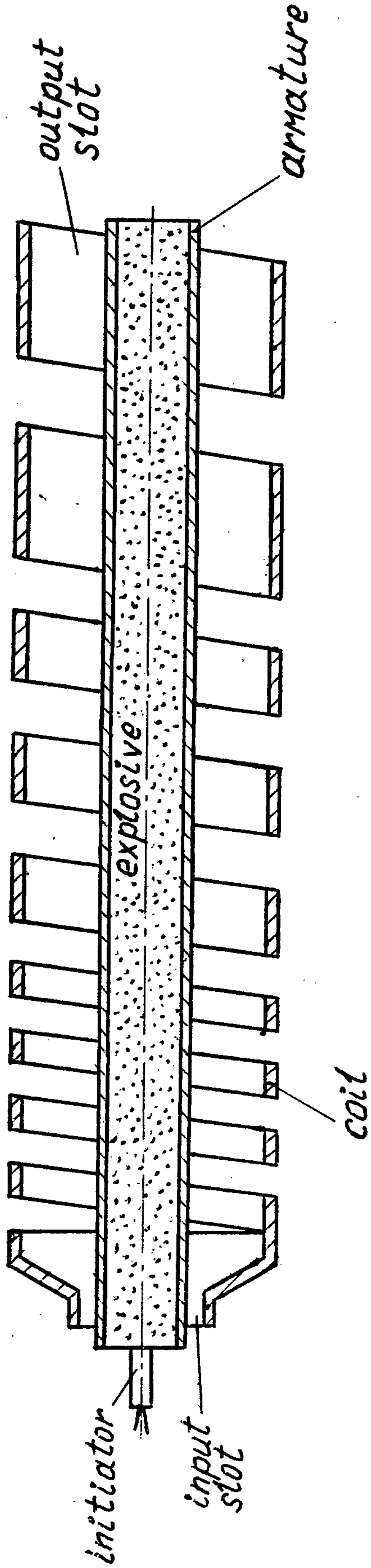

Fig. 29. Helical MC-generator schematic.

$$\omega = \sqrt{\frac{1}{LC} - \frac{R^2}{4L^2}}, \tag{3.3}$$

$$\omega = \omega_0 \sqrt{1-\gamma^2}, \tag{3.4}$$

here

$$\gamma = \frac{R}{2}\sqrt{\frac{C}{L}}, \qquad \omega_0 = \frac{1}{\sqrt{LC}}$$

At the moment of $T_m = \pi/2\omega$ the magnetic flux stored in the contour equals:

$$\varphi = \frac{U_0}{\omega}\exp\left(\frac{-\pi R}{4L\omega}\right) = U_0\sqrt{LC}\exp\left(\frac{-\pi\gamma}{2\sqrt{1-\gamma^2}}\right), \tag{3.5}$$

3.2. PREAMPLIFIER OPERATION ON INDUCTIVE LOAD.

Let us observe the operation of a helical MC-generator with a profiled (up-growing) helix width and axial HE detonation at the end when employed as a preamplifier. Fig. 29 illustrates this generator schematic.

The generators with an axial HE are most effective in HE energy conversion into the liner's energy. Depending on the HE mass ratio to the liner mass, the efficiency varies approximately as it is shown in fig.30.

The generator turn widths are profiled so that with current growth the moving liner (dashed line) performs equal work along all sections over the axis, i.e. helix width is made to be increasing with the current growth at the contact point thus providing a constant magnetic field for the moving liner part.

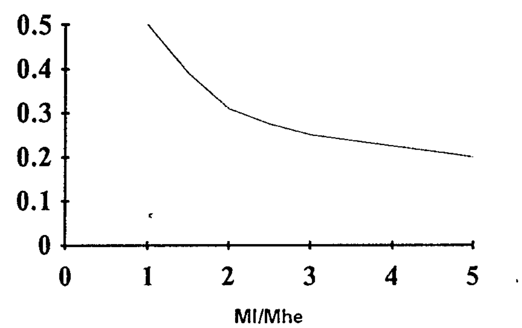

Fig.30. HE energy - liner energy conversion efficiency.

Let the liner accelerated by a HE to velocity V loses the velocity by a magnitude dV when it is decelerated in the magnetic field, then the liner energy ratio is:

$$\frac{W_{H^2}}{W_{he}} = \frac{2\Delta V}{V} - \left(\frac{\Delta V}{V}\right)^2, \tag{3.6}$$

This function can be graphed - fig.31.

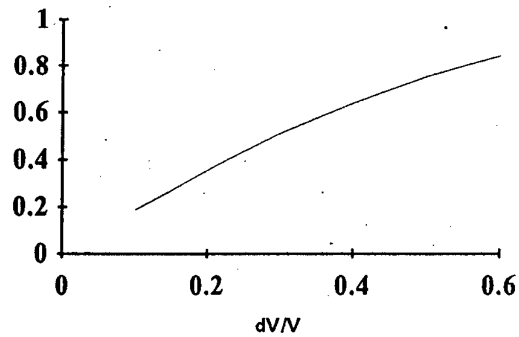

Fig.31. Liner energy transfer efficiency into the magnetic field energy.

As we see, for the effective energy transfer, the liner must be decelerated substantially.

Now let us consider how the magnetic field magnitude suitable for the generator operation depends on its geometrical dimensions. Let a HE be D_{he} in diameter. The liner will be decelerated in the constant magnetic field H at $D_{he}/2$ length. Then the energy imparted to the magnetic field is:

$$W_{H^2} = \frac{\mu_0 H^2}{2}\frac{D_{he}}{2}, \qquad (3.7)$$

the HE energy:

$$W_{he} = \frac{\pi D_{he}^{\ 2}}{4} l_{he}\rho_{he}\omega_{he}, \qquad (3.8)$$

(ω_{he} = 4.2 MJ/kg, ρ_{he} = $1.7 \cdot 10^3$ kg/m).

With Nk efficiency of HE energy transfer to the liner energy and nH efficiency of liner energy transfer to the field energy we obtain the equation:

$$W_{H^2} = \eta_k \eta_h \omega_{he}, \qquad (3.9)$$

or

$$\frac{\mu_0 H^2}{2}\frac{D_{he}}{2} = \eta_k \eta_h \frac{\pi D_{he}^{\ 2}}{4}\rho_{he}\omega_{he}, \qquad (3.10)$$

so we find

$$H = \sqrt{\eta_k \eta_h \frac{\pi D_{he}\rho_{he}\omega_{he}}{\mu_0}} = 10^8\sqrt{1.8\,\eta_k \eta_h D_{he}}\ (\mathrm{A/m}), \qquad (3.11)$$

When HE diameter is less than 0.5, and nK and nH equal 0.5, the magnetic field does not exceed 0.5E8 A/m and the generator operates with small losses in the regime of magnetic field linear diffusion and flux cut-off at the contact point.

Let us have a look at the liner-helix contact point (fig.32).

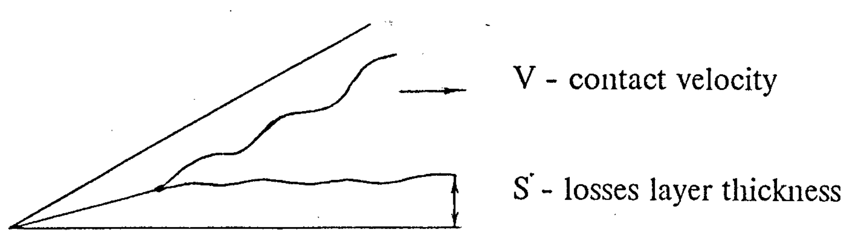

Fig.32. A sliding contact scheme.

At C point there is a sliding contact where the flux is being lost at the velocity (3.9).

$$\dot{\varphi} = 2SV\mu_0 H, \tag{3.12}$$

where V - contact velocity , S - losses layer thickness.

With liner length l, and gap d, the contact point moves at the velocity:

$$V = V_l\, l/d, \tag{3.13}$$

Then
$$\dot{\varphi} = 2SV_l\mu_0 H \frac{l}{d}, \tag{3.14}$$

but $lV_l\mu_0H$ is the generator inductance derivative multiplied by current value $\dot{L}_g I$. Then the flux losses in the contact point are:

$$\dot{\varphi} = \frac{2S}{d}\dot{L}_g I, \tag{3.15}$$

but this expression can be considered as the losses on the contact resistance which equals to:

$$R_c = -\frac{2S}{d}\dot{L}_g, \tag{3.16}$$

With the magnetic field increasing in time according to $H = H_0\exp(t/T)$ law typical of MC-generators, the skin-layer thickness for the magnetic flux is:

$$S_\varphi = \sqrt{\frac{T}{\sigma_0\mu_0}}, \tag{3.17}$$

At T = 100 mcsec typical of MC-generators of this class,
Ro n = 1 mm. Then, at d = 50 mm

$$R_c = -4.10^{-2}\dot{L}_g, \tag{3.18}$$

This value is twice or thrice less than the experimental value:

$$R_c = -0.12\dot{L}_g, \tag{3.19}$$

Additional flux losses can be due to the insulation of 1 mm thickness available between the liner and the turns where the magnetic flux is partially cut off also.

Moreover, highly precise coaxiality for the liner and the helix must be provided, otherwise the contact point jumps from one turn to another and cuts off the flux captured between these two points.

Let us observe now the preamplifier operation on the inductive load with flux losses account in the following form:

$$R_c = -\gamma\dot{L}_g, \tag{3.20}$$

Circuit equation will be written in the form:

$$\dot{\varphi} - \gamma\dot{L}_g I = 0, \tag{3.21}$$

Let us divide this equation by $\varphi = L_g I$. We will have:

$$\frac{\dot{\varphi}}{\varphi} = \gamma\frac{\dot{L}_g}{L_g}, \tag{3.22}$$

With integration over time we obtain the solution:

$$\varphi/\varphi_0 = (L/L_0)^\gamma, \tag{3.23}$$

or

$$I/I_0 = (L/L_0)^{\gamma-1}, \tag{3.24}$$

where γ is of 0.1-0.13 order.

With the considerable inductance variation (10^2-10^3), typical of the preamplifiers, the generator current grows by 50-350 times correspondingly, at high enough coefficient of magnetic flux conservation 0.5-0.35. The generator energy increases by 25-120 times, respectively.

3.3. "HIGH-SPEED" MC-GENERATOR OPERATION ON OPENING SWITCH.

There exist several types of MC-generators with short operation time which can be used to power an explosive plasma opening switch. They are looped, helical, coaxial and disk MC-generators with simultaneous HE initiation along the axis. In all these generators the efficiency of HE energy conversion in the liner energy is rather high and approximately equal, however they differ substantially in the efficiency of their energy conversion into the magnetic field energy. Thus, looped generators have large losses because a liner there should necessarily be longer than a turn width. In helical and coaxial generators the end losses are minimal, and their efficiency is the highest. In disk MC-generator of short operation time the magnetic field pressure is proportional to $1/R^2$, and a HE thickness is proportional to radius R, finally the HE energy use efficiency decreases with radius increase as $1/R^3$. In our experiments the problem of HE energy use efficiency is very important as with increase in mass one must extend the distance to the armor, that correspondingly leads to the increased energy transportation line inductance. For this reason we shall consider only two types of the most effective generators: helical and coaxial with simultaneous HE initiation along the axis.

Let us observe plasma explosive opening switch powered by a helical-coaxial MC-generator as it is shown in fig.33.

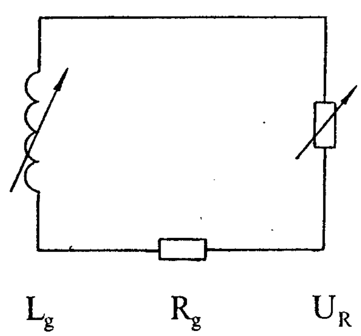

Fig.33. Explosive plasma opening switch powering scheme with a MC-generator.

In the powering process the opening switch voltage remains practically constant. To describe the flux losses on the opening switch we can introduce characteristic time

$$T_R = \frac{\varphi}{U_R}, \qquad (3.25)$$

where φ - magnetic flux in the powering circuit.

Circuit equation for the fig.33 can be written in the form.

$$\dot{\varphi} - \gamma \dot{L}_g I + U_R = 0, \qquad (3.26)$$

Let us divide the equation by φ = L*I

$$\dot{\varphi} - \gamma \dot{L}_g / L + U_R / \varphi = 0, \qquad (3.27)$$

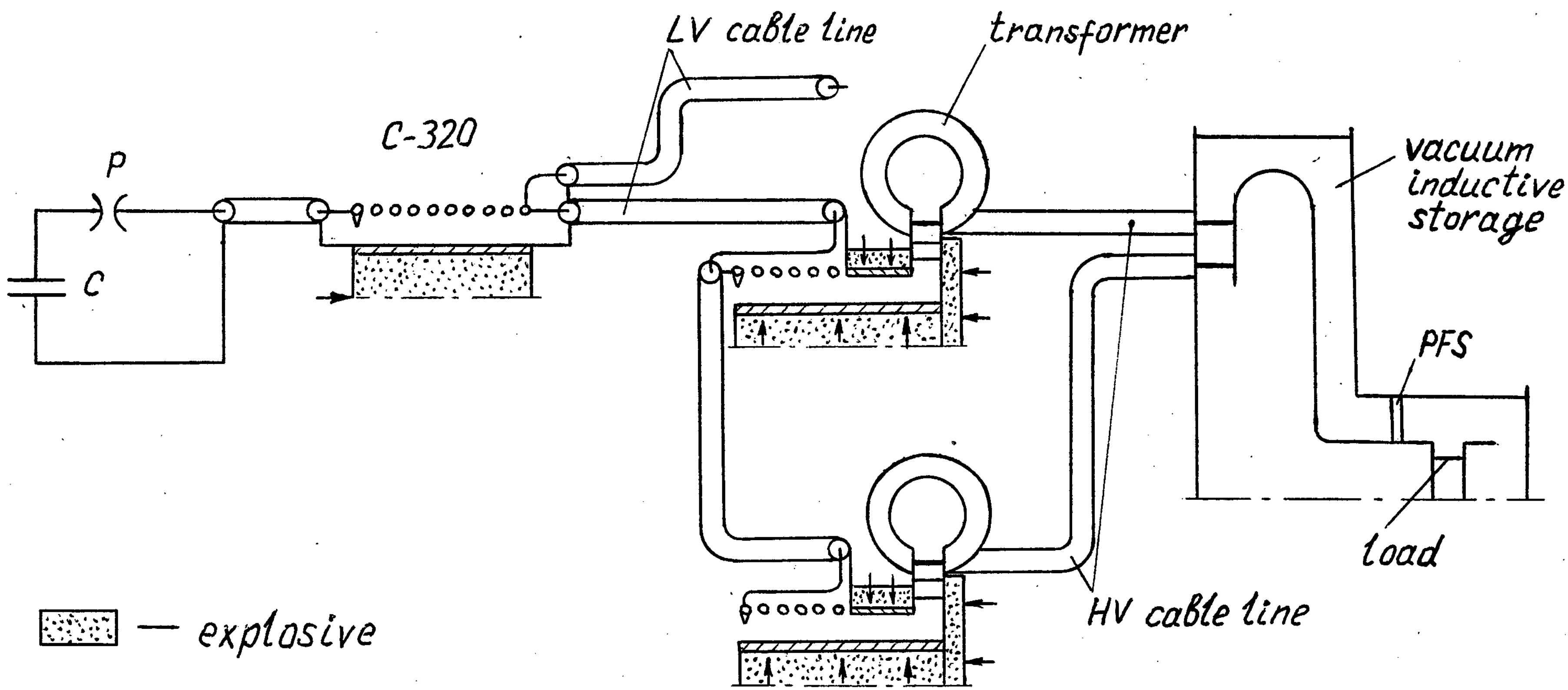

Fig. 34. General scheme for all system components coupling.

Let us integrate accounting that

$$U_R / \varphi = 1 / T_R, \qquad (3.28)$$

then

$$\ln(\varphi/\varphi_0) - \gamma \ln(L/L_0) + t/T_r = 0, \qquad (3.29)$$

Hence, we find the law for current variation :

$$\frac{I}{I_0} = \left(\frac{L}{L_0}\right)^{\gamma-1} \exp\left(\frac{-t}{T_R}\right), \qquad (3.30)$$

In this case the energy is dissipated in the plasma channel of the opening switch:

$$W_{R_0} = \int_0^T I(t) U_R dt \approx \frac{I_0 U_R T}{\gamma}\left(\frac{L}{L_0}\right)^{\gamma}, \qquad (3.31)$$

4. CALCULATED OPERATION FOR FOUR HELICAL-COAXIAL GENERATORS TO PROVIDE 60 MA CURRENT IN PFD.

Fig.34 gives a general coupling scheme for all components in the MC - generator system employed for PFD powering to 60 MA current.

The PFD chamber of 6 nH inductance is powered via a high - voltage cable line comprising 200 KVI-300 cables 8 m long and of 6 nH inductance by four helical - coaxial generators with step-up transformers of 4-fold transformation coefficient.

Each helical - coaxial generator has 160 nH initial inductance in the helical section and 20 nH in the coaxial section. One helical generator C-320 powers generators in series - parallel pattern 2x2 as shown in fig.35.

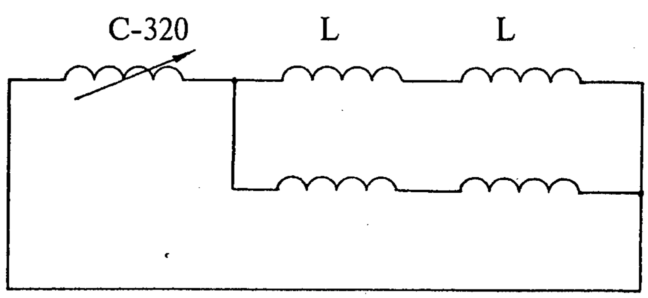

Fig.35 series - parallel scheme for helical - coaxial generator powering.

The cable line inductance in single generator powering is 140 nH so the total inductance of the series - parallel generator coupling with the cable line is 300 nH.

Helical generator C - 320 of 12.5 μH initial inductance is powered with 350 kA initial current by a capacitor bank (C = 6 mF, U = 20 kV) or by cascade generators C-80, C-160. In 200 mcsec the C- 320 generator produces 10 MA current and 15 MJ energy on 300 nH inductive load.

At the powering stage 5 MA current flows in each helical - coaxial generator helix. At the generator HE detonation and explosive plasma opening switch contour closure by a liner, the magnetic flux is ousted on the coaxial inductance and the parallel inductance of the generator powering line. By the end of the coaxial section operation the coaxial current reaches 27 MA with a total coaxial and opening switch inductance of 22 nH. By this moment the inner HE is detonated along the axis, and outer HE is initiated over the surface.

In 5 mcsec the coaxial inductance reduces to 10 nH and the current reaches 45 MA. Five microseconds before the end of the generator operation the explosive plasma opening switch starts working where the voltage from ~ 1 kV increases to 60 kV in 0.2 - 0.5 mcsec and during the operation remains practically constant.

In last 5 mcsec the coaxial generator increases the current to 70 MA operating on 6 nH total inductance (the residual generator inductance - 2 nH, transformer inductance - 1 nH, and PFD chamber equivalent inductance - 3 nH).

The cable transformer increases the voltage to 180 kV and decreases the cable line current to 15 MA. All four generator currents are summarized on the vacuum chamber collector and 60 MA current flows in PFD.

CONCLUSION.

Various schemes for plasma flow discharge powering with MC - generator to 60 MA current are considered in part 1. Calculations of the simple powering schemes are done for the inductive storage of the plasma flow discharge via the buffer inductance, slow - operating MC - generator of C - 320 type, and the explosive plasma opening switch.

It was shown that this scheme can be applied in 25 MA current range.

In 60 MA current range to effectively transfer the MC - generator energy to the inductive storage in short time of 5 mcsec order, it is necessary to employ a more complicated scheme with a " high - speed " MC - generator facilitating the magnetic flux ousting to a load in this time period and simultaneous current contour breakage with an opening switch. To provide 60 MA current in the PFD inductive storage one needs four helical - coaxial generators equipped with explosive plasma commutators. And to match their impedance with PFD impedance it is demanded to employ pulsed high - voltage transformers.

REFERENCES

1. 8th IEEE International Pulsed Power Conference, San Diego, California, 1991. R.White and K.Prestwich. Future explosive pulse-power technology for high-energy plasma physics experiments. R.E.Reinovsky, I.R.Lindemuth, and S.P.Marsh. pp. 415-418
2. 8th IEEE International Pulsed Power Conference, San Diego, California, 1991. R.White and K.Prestwich. A compact torus plasma flow switch. Robert E.Peterkin, James H.Degnan, Norman F.Roderic, Carl R.Sovinec and Peter J.Turchi. pp. 277-282
3. 9th IEEE Pulsed Power Conference, Albuquerque, New Mexico , 1993. "EMG-PIRIT" experimental complex for investigations of high energy plasma formations. A.I.Pavlovskii, N.F.Popkov, A.S.Pikar', E.A.Ryaslov, W.I.Kargin, P.V.Mironychev et al.
4. Pavlovskii A.I., Lyudaev R.Z., Kravchenko A.S. et al. In: Megagauss Physics and Technology: Ed. by P.J.Turchi. Plenum Press, NY and L, 1980, p. 595.

5. Pavlovskii A.I., Popkov N.F., Pikar A.S. et al.In: Megagauss Field and Pulsed Power Systems: Ed. by V.M. Titov and G.A.Shvetsov. Nova Science Publishers, NY, 1990, p.503.
6. Pavlovskii A.I., Lyudaev R.Z., Zolotov V.A. et al. In: Megagauss Physics and Technology: Ed. by P.J.Turchi. Plenum Press, NY and L, 1980, p. 557.
7. Pavlovskii A.I., Lyudaev R.Z., Sel'chenkov L.I. et al. In: Megagauss Physics and Technology: Ed. by P.J.Turchi. Plenum Press, NY and L, 1980, p. 585.
8. Degnan J.H., Baker W.L., Fowler C.M. et al. In: Ultrahigh Magnetic Fields. Physics. Techniques. Applications: Ed. by V.M. Titov and G.A. Shvetsov. Moscow, Nauka, 1984, p.352.
9. Reinovsky R.E., Lindemuth I.R., Goforth J.H. et al. In: Megagauss Field and Pulsed Power Systems: Ed. by V.M. Titov and G.A.Shvetsov. Nova Science Publishers, NY, 1990, p.453.
10. Pavlovskii A.I., Lyudaev R.Z., Boyko B.A. et al. In: Megagauss Field and Pulsed Power Systems: Ed. by V.M. Titov and G.A.Shvetsov. Nova Science Publishers, NY, 1990, p.233.
11. Pavlovskii A.I., Vasyukov V.A., Russkov A.S. Pis'ma v JTF, V.3, N.16, 1977, p.789.
12. Pavlovskii A.I., Vasyukov V.A., Popkov N.F. et al. In: Ultrahigh Magnetic Fields. Physics. Techniques. Applications: Ed. by V.M. Titov and G.A. Shvetsov. Moscow, Nauka, 1984, p.410.
13. Pavlovskii A.I., Babich L.P., Mironychev P.V., and Shmorin I.T. In: Megagauss Field and Pulsed Power Systems: Ed. by V.M. Titov and G.A.Shvetsov. Nova Science Publishers, NY, 1990, p.509.
14. Caird R.S., and Fouler C.M. In: Megagauss Technology and Pulse Power Applications: Ed. by C.M.Fouler, R.S.Caird, and D.J.Erickson. Plenum Press, NY and L, 1987, p.425.
15. Knoepfel H. Pulsed High Magnetic Fields. Amsterdam: North-Holland, 1970.